H. Hobæk, On vertical echo sounder bottom echoes, Proceedings of the 34^{rd} Scandinavian Symposium on Physical Acoustics, Geilo, Norway, January 30 - 2 February, 2011

On vertical echo sounder bottom echoes

Halvor Hobæk
Department of Physics and Technology
University of Bergen, Norway
e-mail: halvor.hobak@ift.uib.no

Abstract

In two previous presentations in this series of symposia we have discussed the validity of depth correction of echoes suggested by Poliquen [1]. This is a sequel in order to rectify a minor assumption in the theory and add results from a series of experiments on plane reflectors. The conclusion remains: the scaling of echoes in order to correct for different depths is not relevant.

1 Introduction

The main assumption in Poliquen's model for depth correction is that the echo from the bottom in a vertical echo sounder increases with depth due to the extra time the outskirts of the beam need to hit the bottom. This was discussed in detail in [2,3]. In brief, the echo length should be proportional to a coefficient depending on the beamwidth only. The interest for making depth corrections to the echo comes from attempts to utilize the trailing part of the echo to reveal information on the bottom parameters, such as roughness and presence of seagrass.

In [2] a simple theory to describe the details of the vertical incidence echo from a plane horizontal bottom was outlined, and further developed in [3]. It was later discovered that it was also necessary to include contributions due to the normal derivative of the directivity function at the bottom interface, which is presented below. It turned out to be insignificant after all. Further, as discussed in [3], the simulations assume and results in waveforms of pressure while both the transmitted signal and the received echo pass through a rather narrowbanded transducer. So, in order to compare simulations and experiments one should compensate for the transfer function of the transducer. Attempts to do so are presented below.

In [3] measurements of echo lengths from a plane copper disk were presented, but only for a limited range of depths. Supplimentary experiments for a larger range of depths are shown below, both for the plane copper disk and the same covered with a thin layer of sand particles, attempting to represent random scatterers on a plane.

Finally, a discussion of the appropriate reflection coefficient to use in the simulations is included, together with measurements of echo amplitude as a function of incidence angle, both for the plane copper disk and the sand covered disk.

2 Theory

In [3] a preliminary simulation model was presented, based on the Helmholtz integral and the Kirchhoff approximation (i.e. using the incoming pressure instead of the total pressure under the integral). This model differs somewhat from Poliquen *et al.*[1], where the reflected field is calculated from the Rayleigh integral after obtaining the velocity at the interface from normal impedance relations. Moreover, they calculated the reflected intensity, while the present model calculates the pressure. A brief resumé of the theory follows. The Helmholtz integral is

$$p(\mathbf{r}) = \int_S (G\nabla_0 p(\mathbf{r}_0) - p\nabla_0 G) \cdot d\mathbf{S},$$

where the surface S is the plane bottom closed by a semispherical surface extending to infinity, and the gradients are taken normal to the surface.

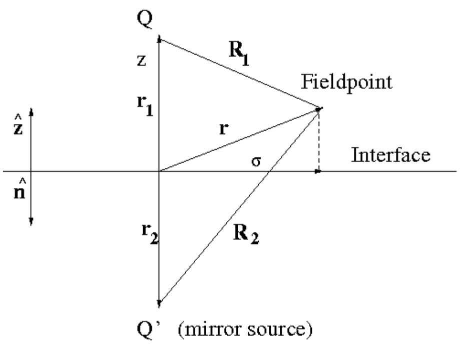

Figure 1: Geometry

The Greeens function is (see Figure 1)

$$G(\mathbf{r}, \mathbf{r}_1) = \frac{e^{ikR_1}}{4\pi R_1} + \mathcal{R}\frac{e^{ikR_2}}{4\pi R_2},$$

where $R_1 = |\mathbf{r} - \mathbf{r}_1|$ and $R_2 = |\mathbf{r} - \mathbf{r}_2|$, as shown in Figure 1. $\mathcal{R}$ is the reflection coefficient, and k the wave number. At the interface this gives

$$G(\mathbf{r}, \mathbf{r}_1)|_{z=0} = (1 + \mathcal{R})\frac{e^{ikR}}{4\pi R}$$

and

$$\nabla G = \cos\phi \frac{e^{ikR}}{R}(ik - \frac{1}{R})(\mathcal{R} - 1)\hat{\mathbf{z}},$$

where $\cos\phi = z_1/R$, $\hat{\mathbf{z}}$ is the unit vector in the $z-$direction (pointing into the fluid), and $R = R_1 = R_2$. The incident pressure is

$$p_{inc} = p_A \frac{A}{R} D(\sigma) f(R - ct)$$

in terms of the pressure amplitude p_A at a distance A from the source with directivity function D expressed in terms of σ, the distance from nadir along the interface, and the wave burst shape, $f(R-ct)$. c is phase velocity and t time. It is tacitly assumed that the wave is narrow-banded in frequency so that a monochromatic Greens function can be applied. New in the model is that ∇p_{inc} also needs to account for the normal derivate of $D(\phi)$. This gives: $\nabla p_{inc} = p_A\{D'\frac{f}{R} + \cos\phi D(\sigma)\frac{A}{R^2}[Rf' - f]\}(-\hat{\mathbf{z}})$ where $f' = \frac{df(R-ct)}{d(R-ct)}$ is the derivate of the wave shape, and $D' = \frac{\partial D}{\partial \phi}\frac{\partial \phi}{\partial R}$ the derivate of the directivity function. The solution is now written as the convolution between a kernel and a function of the burst (ff):

$$kernel = \cos\phi D \frac{e^{ikR}}{R^2}\, dR$$

$$ff = -A_2 D' f + D(A_1 f - A_2 f')$$

where $A_1 = 2\mathcal{R}\frac{1}{R} - ik(\mathcal{R} - 1)$ and $A_2 = 1 + \mathcal{R}$. Note an extra D in the kernel to account for directivity on reception.

In practice the $A_2 f'$ term in ff dominates strongly over the first term. The new term (the first) turns out to have negligible influence on the result!

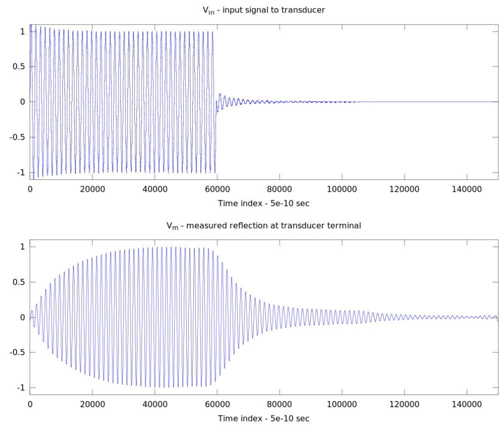

Figure 2: Signal input to transducer and output from the transducer of echo by a plane reflector

In [3] we used a rectangular burst (a certain number of whole cycles) or a burst measured with a probe with rectangular burst input to the source. This time a different approach is used: we apply the *convolution theorem* on the impulse response of the transducer, g. First we need to find g, as follows: Let V_{in} be the signal input to the transducer, V_m be the signal from the transducer of the echo from the reflector with reflection coefficient $\mathcal{R}$. Then $V_m = (V_{in} * g) * \mathcal{R} * g'$. Here g' is the reciprocal impulse response of the transducer, and $*$ denotes convolution. We assume reciprocity, e.g. $g' = g$, and that $\mathcal{R}$ is independent of frequency, eg. constant (=1). Thus, $V_m = V_{in} * (g * g)$ or, $FT(V_m) = FT(V_{in})FT(g * g) = FT(V_{in})FT(g)^2$, where FT denotes Fourier transform. Hence, $FT(g) = \sqrt{(FT(V_m)/FT(V_{in}}$. Finally, the waveform in water is found by

$$Ws = IFT\{FT(g)FT(V_{in}\},$$

where IFT denotes inverse FT.

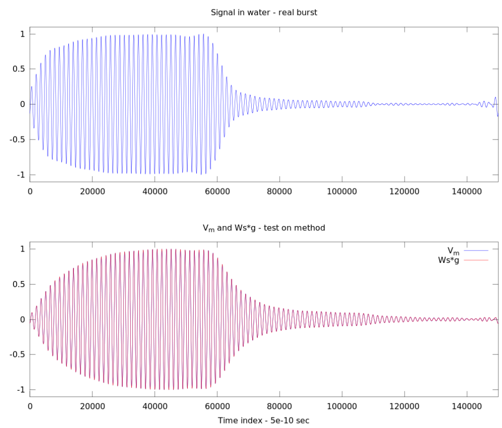

Figure 3: Upper panel: Resulting "water signal" (pressure). Lower panel: convolution of water signal and impulse response, and measured signal.

Figure 2 shows the signal input to the transducer, and the output from the transducer of the echo from a plane reflector at suitable distance,V_m, (both are filtered and normalized), e.g. the signals needed for computing the impulse response of the transducer.

The upper panel of Figure 3 shows the resulting water signal, W_s, used in the simulations. The lower plot is a test: It shows the measured echo, V_m, and W_s convolved with the impulse response g, plotted on top of each other.

Convolving the measured signal V_m once more with the impulse response g makes negligible difference. The reason becomes apparent by examining the spectrum of g. It represents the bandpass of the transducer, and modifies the signal very little, see Figure 4.

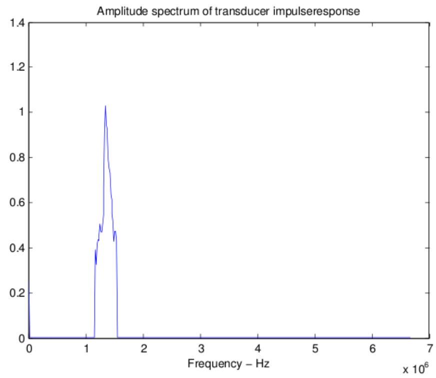

Figure 4: Amplitude spectrum of transducer impulse response

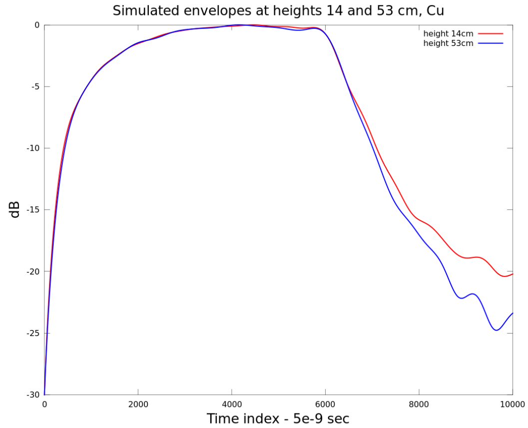

Figure 5: Simulated echoes at 14 and 53 cm depth of copper reflector.

2.1 Simulations

Applying the ordinary plane wave reflection coefficient for a water-Cu interface, Figure 5 shows envelopes of simulated bursts at 14 and 53 cm depth, respectively. There is little difference to be seen between the two echoes.

In Figure 6 burst lengths versus depth are plotted. Here also measured burst lengths are included (see below).The burst lengths are determined at several levels beneath the maximum envelope amplitude. Also here there is no systematic variation of burst length with depth. If reflection coefficient is put constant, e.g. independent of incidence angle, very little change is seen, but is not shown here.

3 Experiment

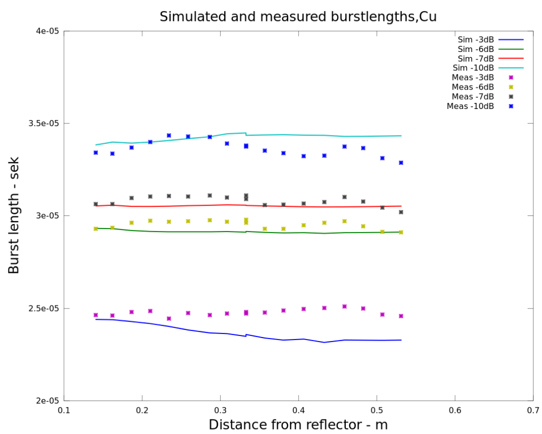

Figure 6: Simulated and measured burst lengths, Copper reflector.

The experiment was based on standard equipment, Figure 7. A function generator provides the bursts fed to the transducer. The received echo (from the same transducer) is recorded on a digital oscilloscope and transferred to a PC for further analysis. The reflector is placed on the bottom of the tank and the transducer can be positioned at heights up to about 70 cm above. The transducer and the reflector can be tilted about horisontal axes which are perpendicular to each other to ensure normal incidence of the beam axis.

The transducer is a disk of PZT of effective radius 3.4 ± 0.4 mm, with a θ_{-3dB} angle $= 4.6^o$ and Rayleigh distance 3.3 cm at 1.35 MHz, inserted in a brass baffle. The first sidelobes are at about 16^o and lie about 30 dB below the main beam. The reflector is a polished 5 cm thick copper disk of diameter 20 cm. It is a good candidate for a plane reflector with reflection coefficient $\mathcal{R} = 0.932$. Measurements were also taken with the reflector covered with a mixture of coarse and fine sand, attempting to represent random scattering.

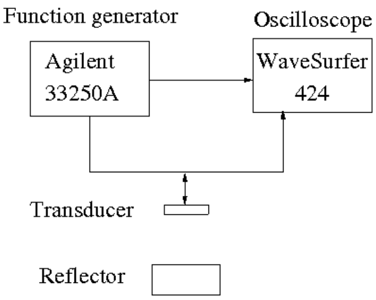

Figure 7: Experimental setup.

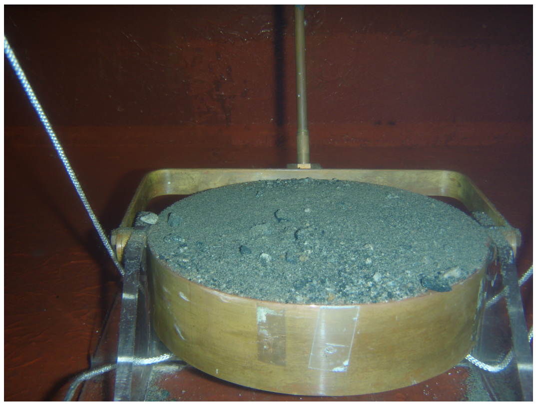

Figure 8: Copper disk reflector with sand layer.

3.1 Results

Results from measurements on the copper reflector are already presented with the simulations. Figure 9a shows a sample echo taken at the shallowest depth (14.1 cm), with the raw signal (red), filtered signal (green) and the resulting envelope (blue) superimposed. The similar signals for a depth of 53.1 cm is shown in Figure 9b.The arrival time is found by locating the front of the echo envelope at half its maximum amplitude, and the length of the echo by the tail of the echo at the same amplitude.

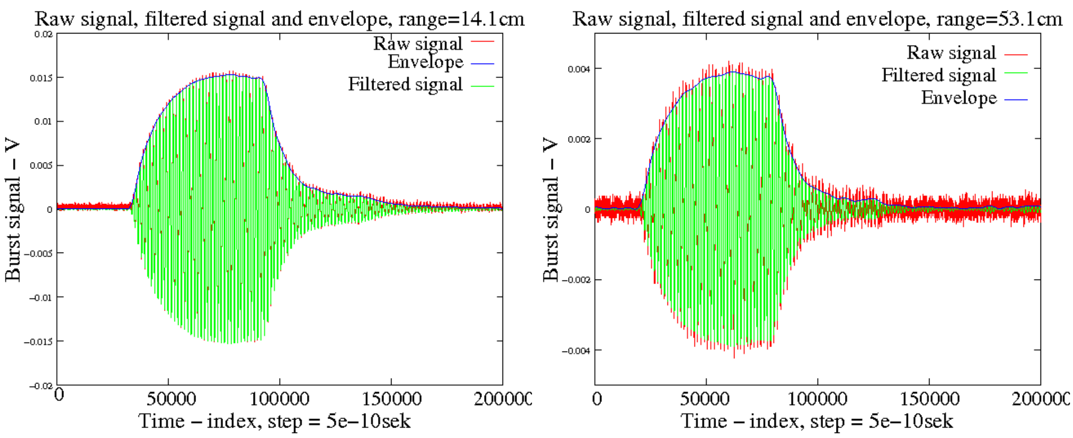

(a) (b)

Figure 9: a) Echo at short range, sand on Cu. b) Echo at long range, sand on Cu.

Neither the shape or the length of the echoes differ much it these two examples. In Figure 10a envelopes at 4 different depths are plotted together. Only in the deeper parts of the tail of the echoes we can see differences. Figure 10b shows echo lengths versus depths determined at 4 different levels below the maximum envelope amplitudes. It is obvious that the echo length is independent of the depth.

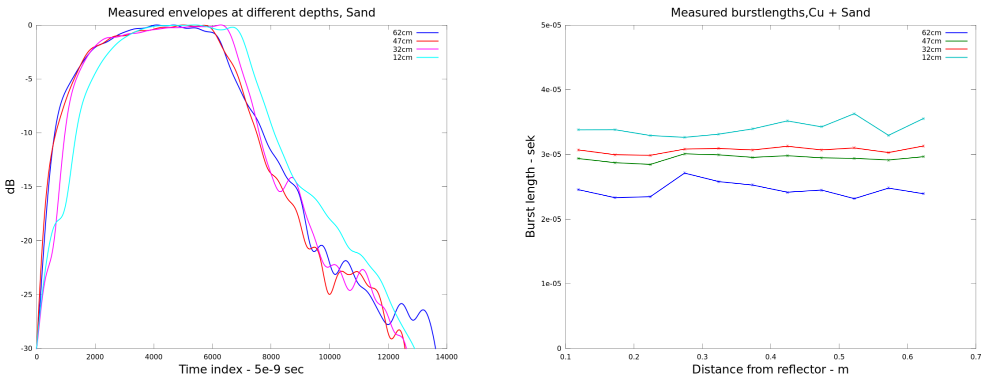

(a)

(b)

Figure 10: a) Echo envelopes at different depths. Sand on Cu. b) Echo lengths versus depths. Sand on Cu.

3.2 Reflection coefficient

In agreement with previous findings in [3] it is obvious that neither with the plane reflector, nor with the sand covered reflector does the echo length or shape change with depth. This is also confirmed by the simulations, assuming the reflection coefficient to be either constant or to be the plane wave reflection coefficient. This indicates that the dominant contribution to the echo comes from nadir alone (i.e. the bottom area just below the transducer), and that the ringlike areas outside nadir has very little importance. This is also indicated by the simulations, which are almost insensitive to the type of reflection coefficient used.

In [3] the reflection coefficient was discussed without reaching any conclusion. The plane wave reflection coefficient is obviously not correct to use here, since it gives the amplitude of the wave reflected in the specular direction, not for the backpropagating wave, except for waves of normal incidence. In our case the wave is not plane but a beam, and only the parts closest to the axis will be reflected back to the source. A contrast to this is when the reflector is covered with sand. In practice, each grain of sand acts as a random scatterer, and one should expect as a first approximation that the reflection coefficient would be almost independent of direction. If so, the echo length ought to be depth dependent - which we have found not to be the case.

(a) (b)

Figure 11: a) Plane wave reflection = Specular reflection. No other directions predicted. b) Simplified assumption: uniform scattering in all directions, e.g. $\mathcal{R} = const$.

In [4] reflection properties are briefly discussed, and the examples in Figure 12 show 2 extremes which may be found in practice. It is, however, unclear what are the conditions to have the "backscatter enhancement" shown in panel b). In the simulatioins we have tried other models for reflection: Lambert's law (intensity goes as cosine of incidence angle), Gouraud shading (a variation of Lambert's law), and Taraldsen's reflection coefficient for spherical waves [5]. None of these made any significant change in the simulations.

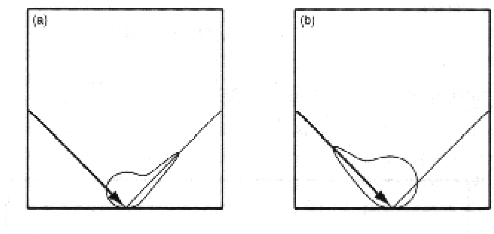

Figure 12: Polar plot of hypothetical scatter with an incident plane wave from left. a) Typical seafloor scattering: peak in the specular direction. b) Backscatter enhancement - no peak in the specular direction. (After [4]).

In order to investigate reflection properties of the copper reflector alone, and copper covered with sand, a set of measurements were made with the transducer positioned at a fixed, short distance from the reflector, and recording the echo obtained while tilting the transducer. In order to keep the beam inside the surface of the reflector the distance was of order 14 cm, but since the Rayleigh distance of the beam is less than 4 cm we should still be sufficiently into the far field. The result for the copper reflector was rather surprising, as shown in Figure 13a and 13b.

The equivalent distance to the reflector, determined from the arrival time of the echoes, is almost constant up to angles near 16 degrees, from when it increases rapidly, as shown in Figure 14. Also shown is the expected distance along the sound axis to the reflector. This means that reflections from nadir dominates in this angular range. However, the observed amplitude is higher than one should expect from the beam directivity, as demonstrated in figure 13b, where the simulated curve indicates the amplitude expected from the part of the beam hitting nadir. The reasons for this higher amplitude is not yet understood. If the backscattered echo at oblique incidence is coming from ranges outside nadir it should be visible in the equivalent distance, as well as in the shape of the echo. Why the amplitude is higher is therefore a mystery. More work is needed in order to translate such measuremnts into an angular dependent reflection coefficient.

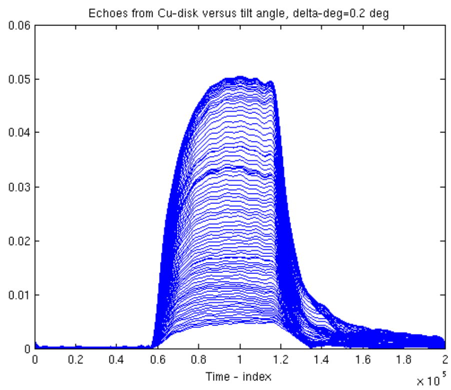

(a)

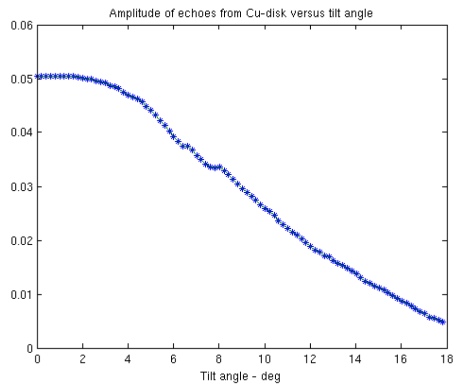

(b)

Figure 13: a) Envelopes of echoes as a function of tilt angle. b) Amplitude of echoes as a function of tilt angle.

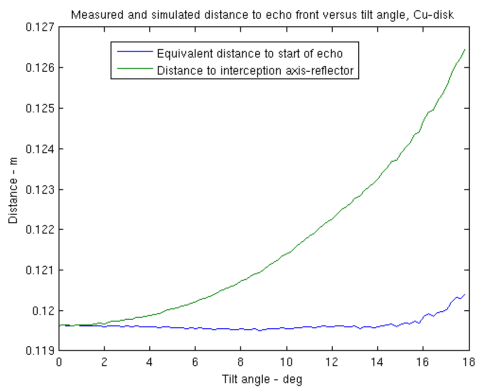

Figure 14: Measured and simulated distance to reflector as a function of tilt angle.

Similar measurements were taken with the sand covered reflector. Here there is a problem with the accuracy of the inclination angle, because of slack in the gear and lack of feedback from the tilting unit. It was impossible to determine the normal incidence angle by looking for the highest amplitude, because of the random scatterers, some of which were rather large. The method used was to adjust for normal incidence with the reflector clean, and then add sand. However, the results look so strange that there is still doubt whether the angles are correct. Examples are shown in Figure 15a - 15b.

The echoes seem to arrive in two groups. The first ones belong to the smaller incidence angles, while the last and largest ones are from angles greater than about 20^o. This is also apparent in the amplitudes. It is possible that normal incidence is near a tilt angle of 5^o in the plots rather than 0^o. As for the plane reflector the amplitude starts to fall off with increasing angle, but at about 16^o it starts to increase again, and reaches a maximum at about 30^o incidence. This may be due to the distribution of the sand grains on the reflector surface, some of which were rather coarse (almost 1 cm diameter). If the assumption of random scattering was correct, the amplitude should fall off monotonically with angle, and the equivalent distance increase. In Figure 16 it is seen to have a big jump (4mm) at about 22^o, which may be due to a big sand grain. Anyway, it is difficult to make any conclusions from these measurements, other than that the monostatic scatter from oblique incidence is a complicated issue.

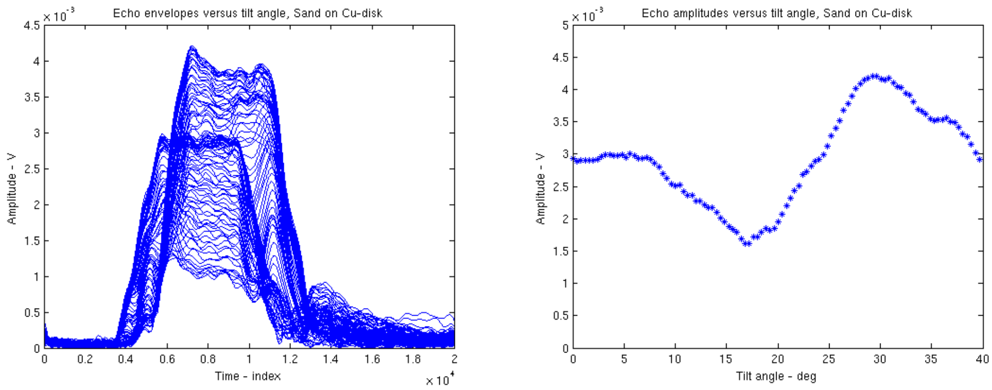

(a) (b)

Figure 15: a) Echo envelopes as a function of tilt angle, Sand on Cu reflector. b) Echo amplitudes as a function of tilt angle, Sand on Cu reflector.

4 Conclusion

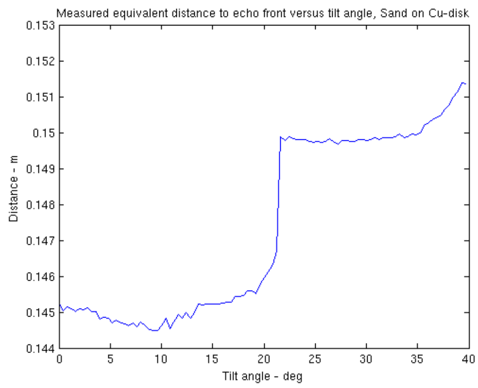

Figure 16: Equivalent distance as a function of tilt angle, Sand on Cu reflector.

The main conclusion is that the normal incidence echoes keep their shape and length as the depth varies. Thus, there is no need to correct for depth dependence. ¡it also seems like information lying in the trailing part of the echo is useless. The important information lies in the arrival time of the echo, and it's amplitude. If the system is calibrated the amplitude can be used to determine the acoustic impedance of the bottom. If the phase of the echo is important, such as to identify if the bottom is soft (gaseous) or hard, one may code the burst, for instance with a chirp, such that the phase can be found by proper decoding (matched filter). If seawood is present it might be possible to detect it by examining the signal just before the main bottom echo. However, here other scatterers, like shools of tiny fish, may complicate the detection.

Regarding the angular dependence of the reflection coefficient it is difficult to draw conclusions from the present measurements.

References

[1] E. Poliquen, "Depth dependence correction for normal incidence echosounding", *Proceings of the Seventh Conference on Underwater Acoustics, ECUA 2004, Delft, The Netherlands, 5-8 July*, 2004.

[2] H. Hobæk and A. Heggen,"Analysis of echoes from a plane reflector - steps towards acoustic habitat mappi ng", in Proceedings of the 32^{th} Scandinavian Symposium on Physical Acoustics, Finse, 2009, R.J. Korneliussen and U. Kristiansen (ed.), p. 106-181, http://www.norskfysikk.no/nfs/faggrupper/akustikk2010/ Proceedings_SSPA2009_Finse.pdf

[3] H. Hobæk and A. Heggen,"On correction of depth dependence for normal incidence echosounders", in Proceedings of the 33^{rd} Scandinavian Symposium on Physical Acoustics, Geilo, Norway,7-10 February 2010, U. Kristiansen (ed.), 9 pages, in http://www.iet.ntnu.no/nb/forskning/groups/akustikk/meetings/SSPA/2010.

[4] D.R. Jackson and M.D. Richardson, *High-Frequency Seafloor Acoustics*, Springer 2007.

[5] G. Taraldsen, "A note on reflection of spherical waves", *J. Acoust. Soc. Am.* **117** (6), 3389-3392 (2005).